Supporting Information

Effect of Rare Earth (RE^{3+}) Ionic Radii on Transparent Lanthanide Tellurite Glass-Ceramics: Correlation between 'Hole-Formalism' and Crystallization

Pritha Patra,[1,2] K. Jayanthi,[3] Margit Fabian,[4] Shweta R. Keshri,[5] Sandip Bysakh,[6] Kaushik Biswas,[1,2] Nitya Nand Gosvami,[5] N. M. Anoop Krishnan,[7] Amarnath R. Allu,[2,8] Kalyandurg Annapurna[1,2,*]

[1] Specialty Glass Division, CSIR-Central Glass and Ceramic Research Institute, 196, Raja S. C. Mullick Road, Kolkata 700 032, India.

[2]Academy of Scientific and Innovative Research (AcSIR), CSIR- Human Resource Development Centre, (CSIR-HRDC) Campus, Postal Staff College Area, Sector 19, Kamla Nehru Nagar, Ghaziabad, Uttar Pradesh- 201 002, India.

[3]ORNL, USA

[4]Centre for Energy Research, 1121, Budapest, Konkoly-Thege st. 29-33, Hungary.

[5]Department of Materials Science and Engineering, Indian Institute of Technology Delhi, Hauz Khas, New Delhi 10016, India

[6]Advanced Material Characterization unit, Material Characterization and Instrumentation Division, CSIR-Central Glass and Ceramic Research Institute,196 Raja S C Mullick Road, 700032, Kolkata, India.

[7]Department of Civil Engineering, Indian Institute of Technology Delhi, Hauz Khas, New Delhi 10016, India

[8]Energy Materials and Devices Division, CSIR-Central Glass and Ceramic Research Institute,196 Raja S C Mullick Road, 700032, Kolkata, India.

*Corresponding authors:

E-mail address: annapurnak@cgcri.res.in(K. Annapurna)

telephone: +91-33-24733496

Fax: +91-33-24730957

Supplementary Information (SI):

1. X-Ray diffraction of RE doped (Ce to Dy) glasses:

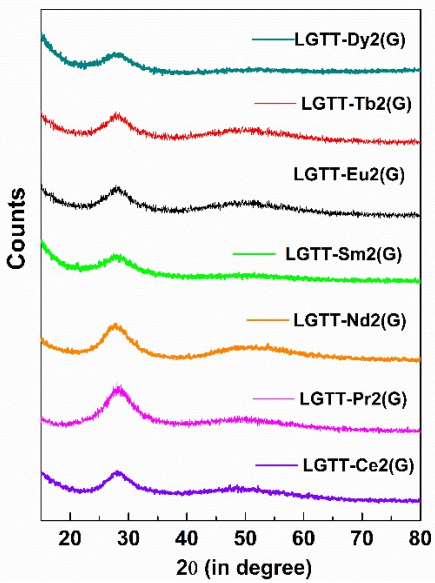

Fig. S1 *X-ray diffraction of all the RE (Ce, Pr, Nd, Sm, Eu, Tb, Dy) doped glasses.*

2. RMC simulation procedure:

For the RMC starting model a random atomic configuration was built up with a simulation box containing 10 000 atoms with density data 0.0636 atomsÅ^{-3} and half-box values r_{max}=26.98 Å for TTLG glass. In the RMC simulation procedure constraints have been used for the minimum interatomic distances between atom pairs (cut-off distances) to avoid unreasonable atom contacts. During the RMC simulations were used coordination constraints for Te, La and Gd surroundings. The starting cut-off distances have been take from previous studies.[37,38,39,40,41] Several RMC runs have been performed by slightly modifying the cut-off distances in the way, that the results of each run have been carefully checked to obtain reliable data for each $g_{ij}(r)$ and coordination number

distributions. For all the samples about 30-35 RMC configurations were obtained with more than 1 400 000 accepted moves of atoms.

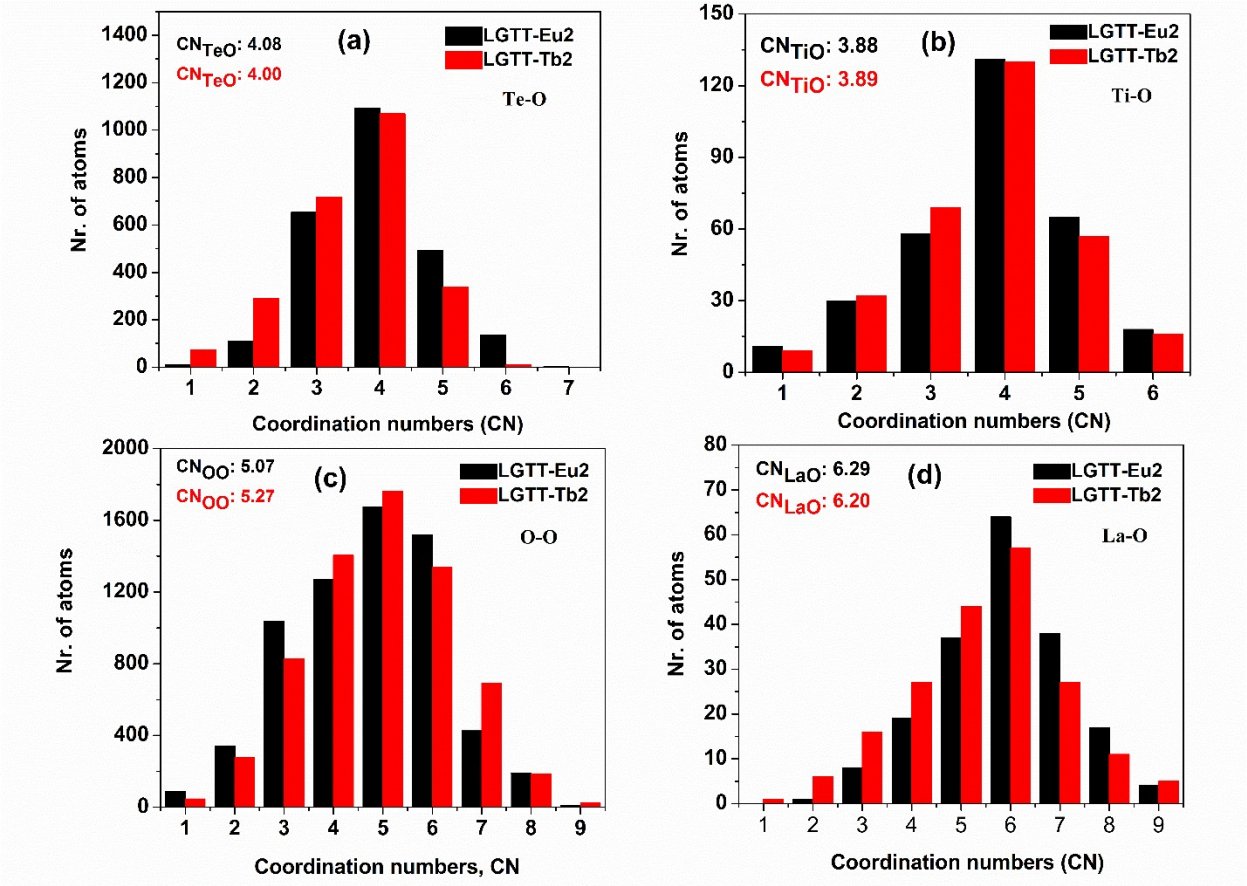

Fig. S2 *Co-ordination numbers (CN) for (a) Te-O, (b) Ti-O, (c) O-O and (d) La-O of LGTT-Eu2 and LGTT-Tb2 glass.*

3. Heat capacity measurement:

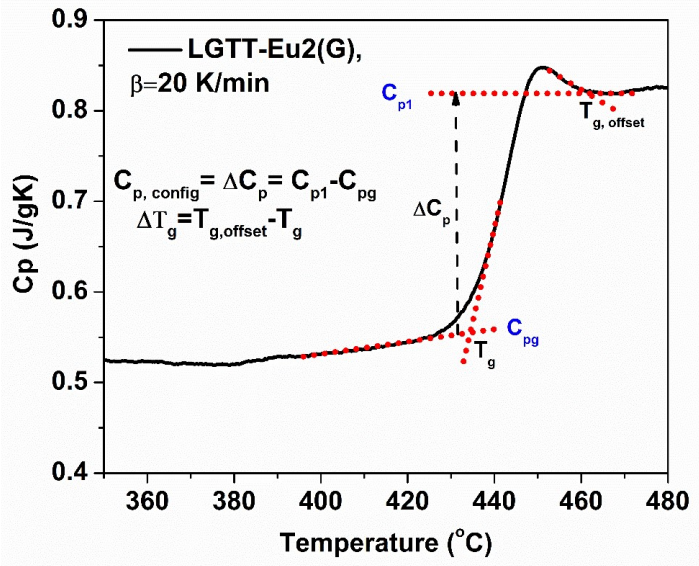

Fig. S3 *The method to identify and calculate T_g, $T_{g,offset}$, ΔT_g and ΔC_p values from Cp curve.*

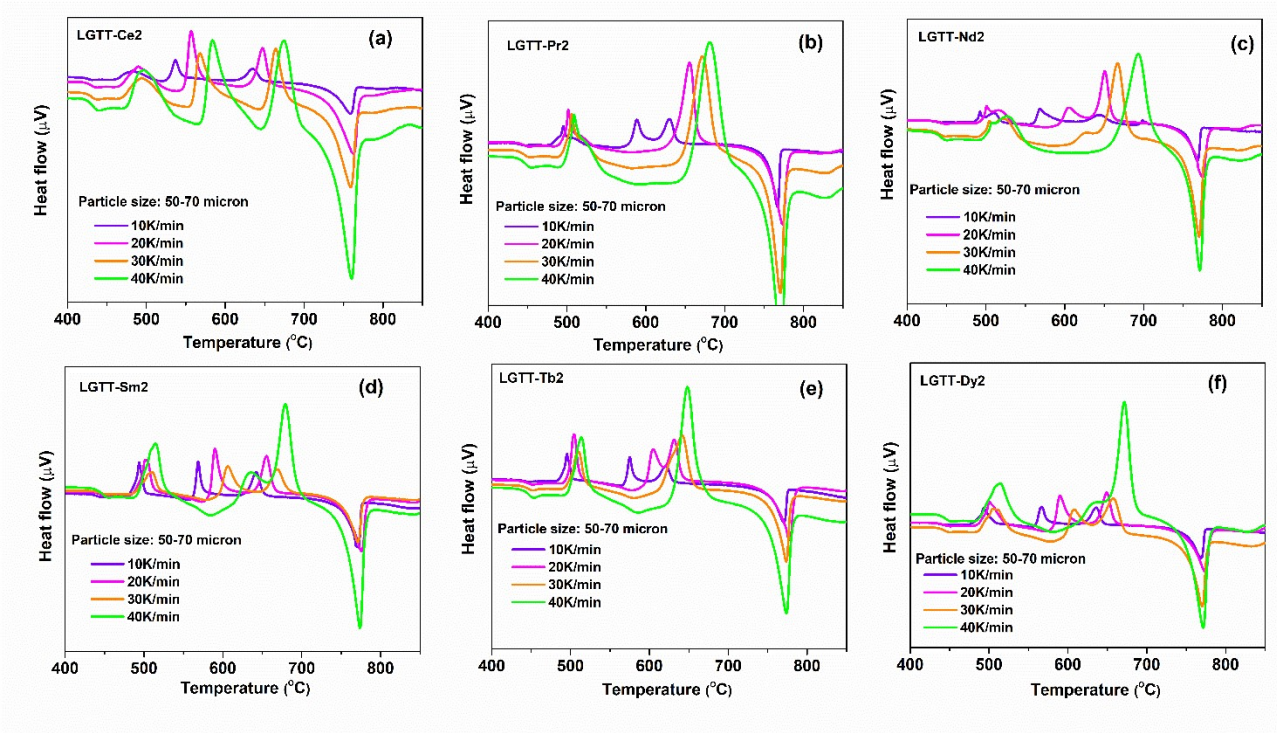

Fig. S4 *DSC thermograms for all the RE doped glasses with four non-isothermal heating rate (β) of 10, 20, 30 and 40 K/min.*

4. Thermal properties of different RE doped (Ce to Dy) glasses:

All the thermal characteristic temperatures like glass transition temperature (T_g), crystallization onset temperature (T_{x1}), first crystallization peak temperature (T_{P1}), melting point (T_m) have been tabulated in Table S1: glass thermal stability ($\Delta T=T_{x1}-T_g$) is calculated using respective T_g, T_{x1}, T_{P1}, T_m values, given in Table S1. For crystallization kinetics study non-isothermal DSC thermograms were recorded at different heating rates (β) of 10, 20, 30 and 40 K/min for all glasses in bulk form under N_2 atmosphere.

Table S1: Glass-transition (Tg, °C), first onset crystallization (Tx1, °C), first crystallization peak (Tp1, °C), melting (Tm, °C), glass thermal stability (ΔT, °C) of LGTT-Ce2, LGTT-Pr2, LGTT-Nd2, LGTT-Sm2, LGTT-Eu2, LGTT-Tb2 and LGTT-Dy2 glasses.

Glass Name	T_g	T_{x1}	T_{p1}	T_m	ΔT
LGTT-Ce2	417	457	482	759	40
LGTT-Pr2	436	476	495	766	40
LGTT-Nd2	433	482	510	768	49
LGTT-Sm2	434	474	494	771	40
LGTT-Eu2	432	475	500	772	43
LGTT-Tb2	435	480	495	771	45
LGTT-Dy2	431	472	492	770	41

Table S2: *Result of the Rietveld refinements of different RE doped LGTT GCs.*

Sample	$(La/Ce\ Gd)_2Te_6O_{15}$		$(La/Pr\ Gd)_2Te_6O_{15}$	
Chemical formula	$(La/Ce)_2Te_6O_{15}$	$Gd_2Te_6O_{15}$	$(La/Pr)_2Te_6O_{15}$	$Gd_2Te_6O_{15}$
Temperature	298 K	298 K	298 K	298 K
Wavelength	1.5458 Å	1.5458 Å	1.5458 Å	1.5458 Å
Crystal system	Cubic	Cubic	Cubic	Cubic
Space group	$Fm\bar{3}m$	$Fm\bar{3}m$	$Fm\bar{3}m$	$Fm\bar{3}m$
GOF	1.47		1.52	
wR	13.97%		15.12%	
Rf^2	15.32%	16.36%	13.7%	11.54%
RF	7.63%	8.56%	12.4%	11.12%

$R = \Sigma||F_o| - |F_c||/\Sigma|F_o|$, $wR = (\Sigma[w(|F_o|^2 - |F_c|^2)^2\ ]/\Sigma[w(|F_o|^4)])^{1/2}$ and $w = 1/(\sigma^2\ (I) + 0.0004I^2)$

Sample	(La/Nd Gd)$_2$Te$_6$O$_{15}$		(La Gd/Sm)$_2$Te$_6$O$_{15}$	
Chemical formula	(La/Nd)$_2$Te$_6$O$_{15}$	Gd$_2$Te$_6$O$_{15}$	La$_2$Te$_6$O$_{15}$	(Gd/Tb)$_2$Te$_6$O$_{15}$
Temperature	298 K	298 K	298 K	298 K
Wavelength	1.5458 Å	1.5458 Å	1.5458 Å	1.5458 Å
Crystal system	Cubic	Cubic	Cubic	Cubic
Space group	$Fm\bar{3}m$	$Fm\bar{3}m$	$Fm\bar{3}m$	$Fm\bar{3}m$
GOF	1.38		1.62	
wR	10.07%		11.56%	
Rf^2	10.52%	11.54%	9.89%	10.25%
RF	13.02%	11.12%	10.58%	10.49%

$R = \Sigma||F_o| - |F_c||/\Sigma|F_o|$, $wR = (\Sigma[w(|F_o|^2 - |F_c|^2)^2]/\Sigma[w(|F_o|^4)])^{1/2}$ and $w = 1/(\sigma^2(I) + 0.0004I^2)$

Sample	(La Gd/Tb)$_2$Te$_6$O$_{15}$		(La Gd/Dy)$_2$Te$_6$O$_{15}$	
Chemical formula	La$_2$Te$_6$O$_{15}$	(Gd/Tb)$_2$Te$_6$O$_{15}$	La$_2$Te$_6$O$_{15}$	(Gd/Dy)$_2$Te$_6$O$_{15}$
Temperature	298 K	298 K	298 K	298 K
Wavelength	1.5458 Å	1.5458 Å	1.5458 Å	1.5458 Å
Crystal system	Cubic	Cubic	Cubic	Cubic
Space group	$Fm\bar{3}m$	$Fm\bar{3}m$	$Fm\bar{3}m$	$Fm\bar{3}m$
GOF	1.77		1.77	
wR	14.19%		14.19%	
Rf^2	11.41%	10.25%	13.89%	13.39%
RF	9.18%	10.49%	12.05%	11.25%

$R = \Sigma||F_o| - |F_c||/\Sigma|F_o|$, $wR = (\Sigma[w(|F_o|^2 - |F_c|^2)^2]/\Sigma[w(|F_o|^4)])^{1/2}$ and $w = 1/(\sigma^2(I) + 0.0004I^2)$

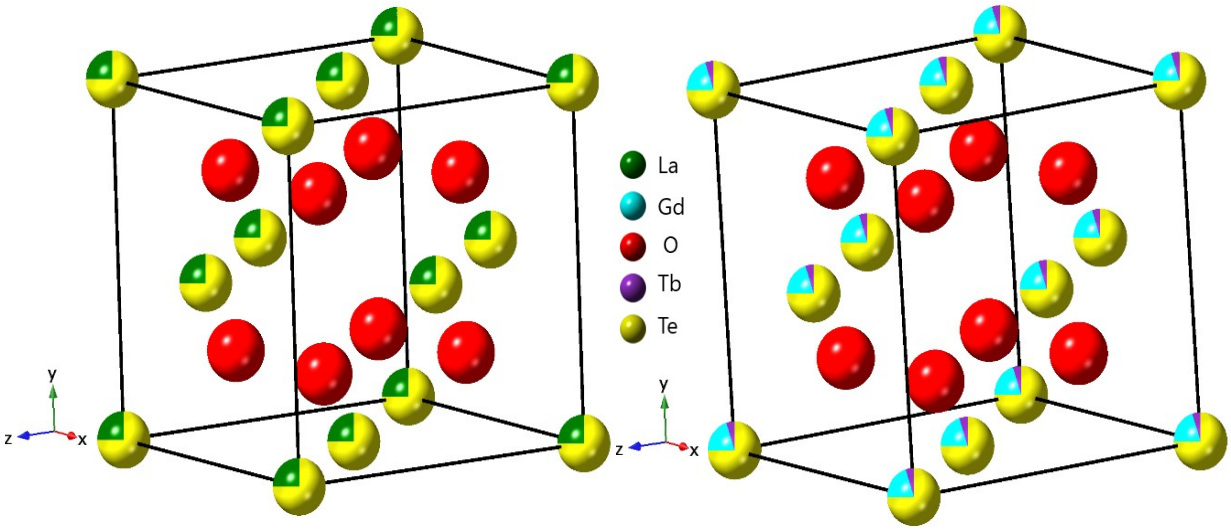

Fig. S5 *Representative crystal structure of $La_2Te_6O_{15}$, and $(Gd/RE)_2Te_6O_{15}$ phases.*

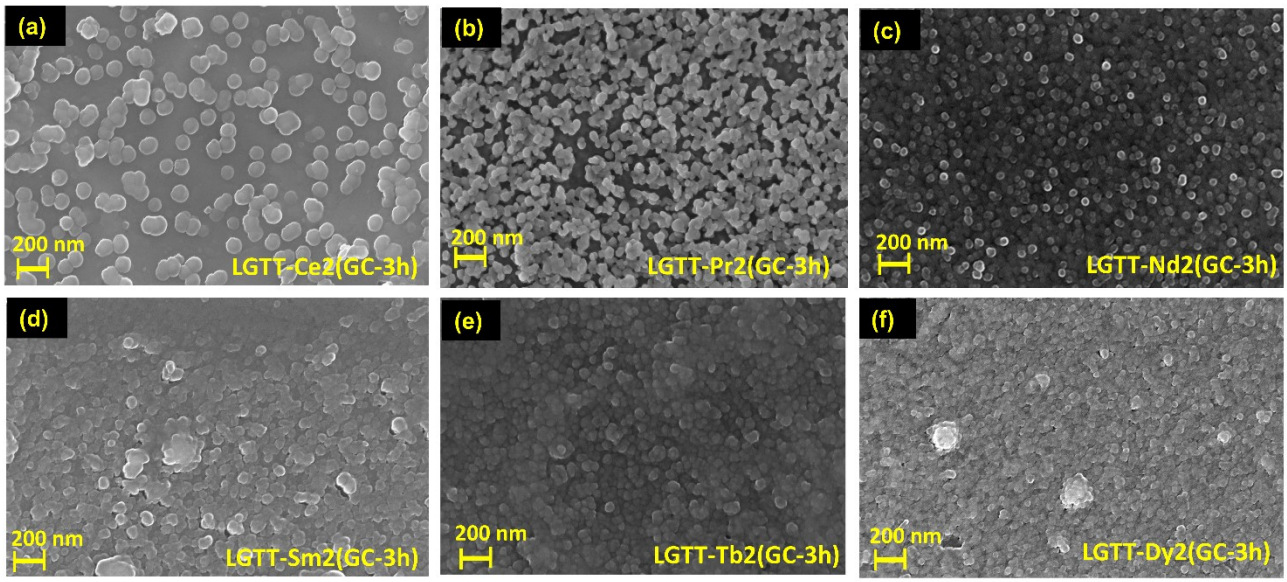

Fig. S6 *FE-SEM images of the 3h heat-treated glass-ceramics (a) LGTT-Ce2(GC-3h), (b) LGTT-Pr2(GC-3h), (c) LGTT-Nd2(GC-3h), (d) LGTT-Sm2(GC-3h), (e) LGTT-Tb2(GC-3h), (f) LGTT-Dy2(GC-3h).*

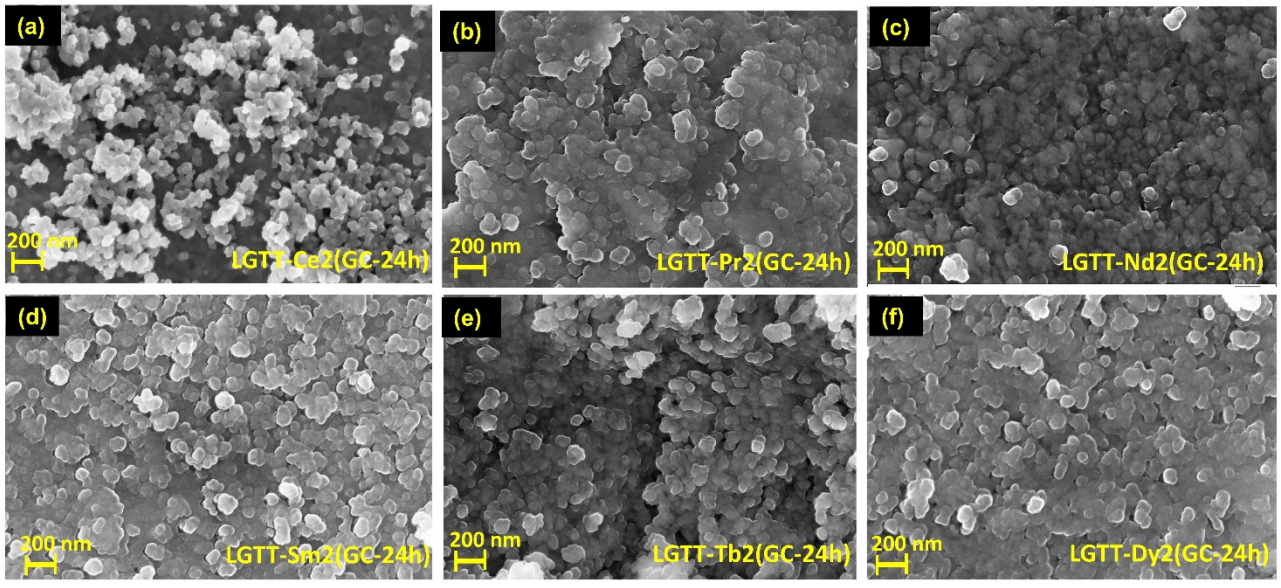

Fig. S7 *FE-SEM images of the 24h heat-treated glass-ceramics (a) LGTT-Ce2(GC-24h), (b) LGTT-Pr2(GC-24h), (c) LGTT-Nd2(GC-24h), (d) LGTT-Sm2(GC-24h), (e) LGTT-Tb2(GC-24h), (f) LFTT-Dy2(GC-24h).*

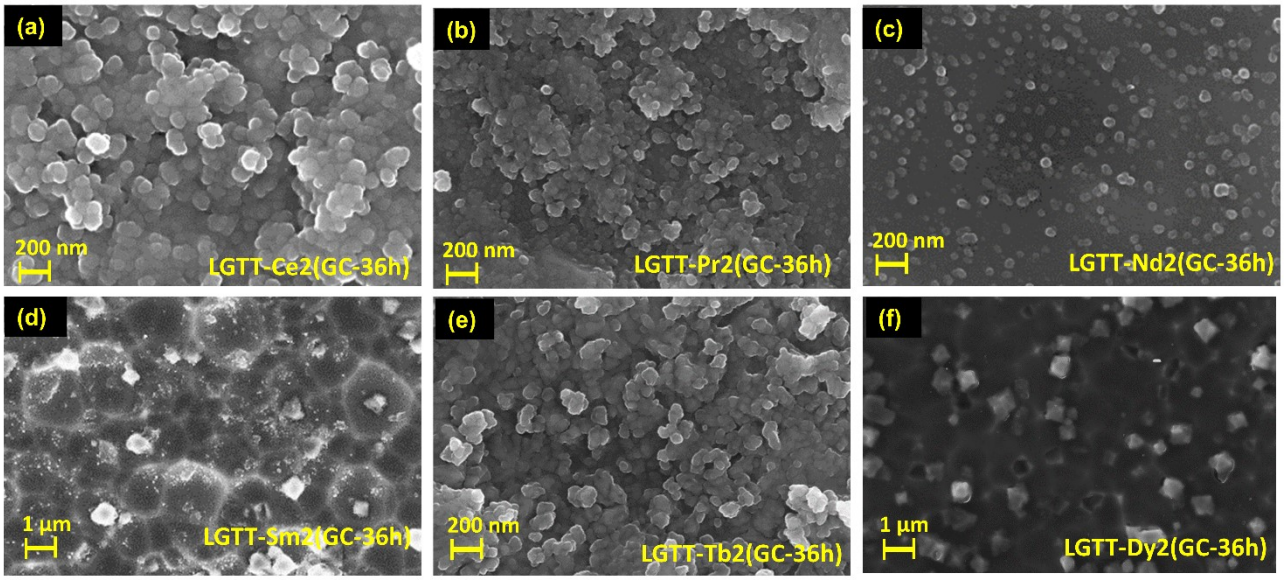

Fig. S8 *FE-SEM images of the 36h heat-treated glass-ceramics after grinding the top surface ~0.5 mm: (a) LGTT-Ce2(GC-36), (b) LGTT-Pr2(GC-36), (c) LGTT-Nd2(GC-36), (d) LGTT-Sm2(GC-36), (e) LGTT-Tb2(GC-36), (f) LFTT-Dy2(GC-36).*

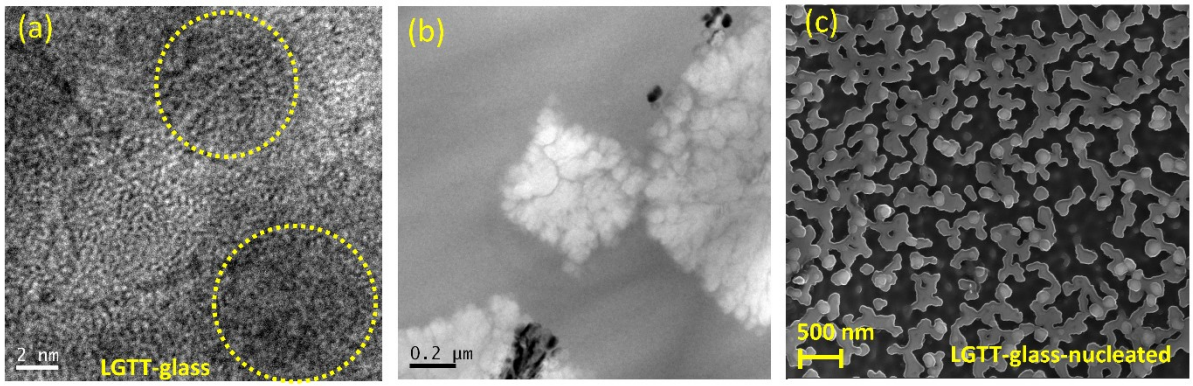

Fig. S9 *(a) HR-TEM image of LGTT-glass (b) BF-TEM image of LGTT-Pr2(GC-36h) (c) FE-SEM image of the nucleated LGTT-glass (at 400 °C).*

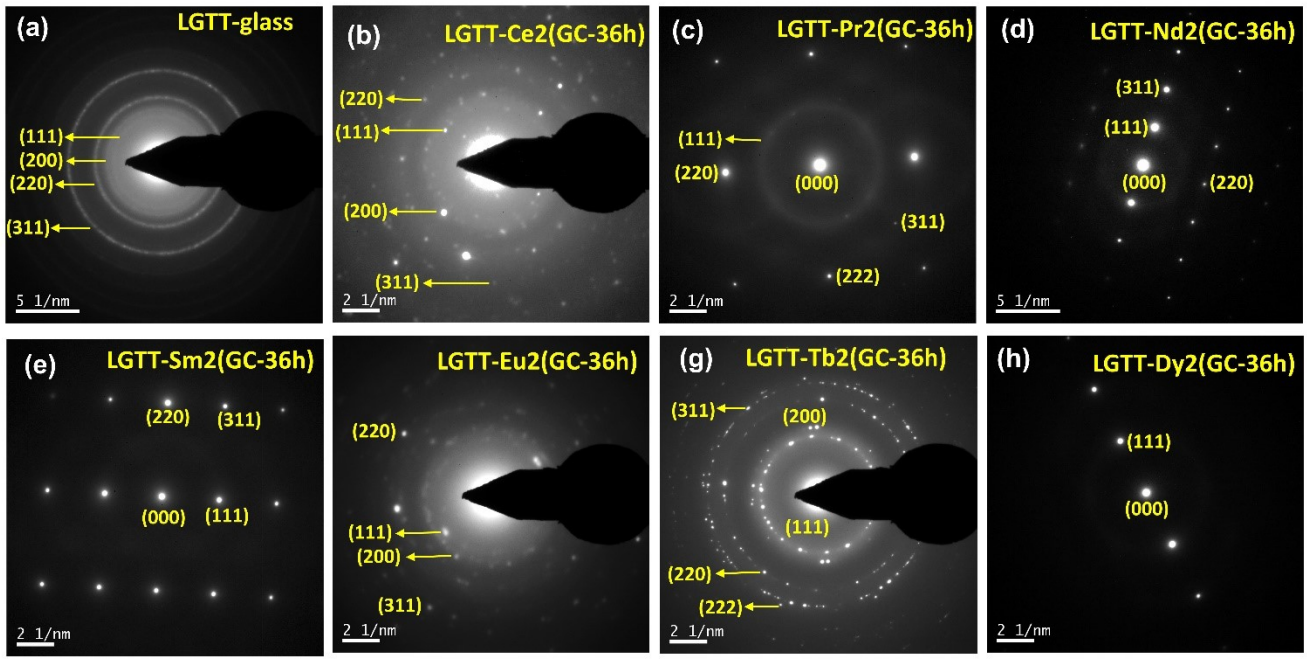

Fig. 10 *SAED-pattern of (a) LGTT-glass, (b) LGTT-Ce2(GC-36h), (c) LGTT-Pr2(GC-36h), (d) LGTT-Nd2(GC-36h), (e) LGTT-Sm2(GC-36h), (f) LGTT-Eu2(GC-36h) (g) LGTT-Tb2(GC-36h) (h) LGTT-Dy2(GC-36h).*